

All-solid all-chalcogenide microstructured optical fiber

Perrine Toupin,¹ Laurent Brilland,² Gilles Renversez,³
and Johann Troles^{1,*}

¹Equipe Verres et Céramiques, UMR-CNRS 6226, Institut des Sciences Chimiques de Rennes, Université de Rennes I, France

²PERFOS R&D Platform of Photonics Bretagne, Lannion, France

³Aix Marseille Université, CNRS, Ecole Centrale Marseille, Institut Fresnel, UMR 7249, 13013 Marseille, France
*johann.troles@univ-rennes1.fr

Abstract: The realization of an all-solid microstructured optical fiber based on chalcogenide glasses was achieved. The fiber presents As₂S₃ inclusions selected as low refractive index material ($n = 2.4$) embedded in a As₃₈Se₆₂ glass matrix ($n = 2.8$). The single mode regime of the fiber was demonstrated both theoretically by multipole method calculations and experimentally by near field measurements. Optical transmission measurements of the microstructured fiber and single index fibers made of the initial glasses reveal an excess of losses as high as 6-7 dB/m. This excess is not due to the guide geometry but can be explained by the presence of defects in the glass interface regions.

©2013 Optical Society of America

OCIS codes: (060.2280) Fiber design and fabrication; (160.2750) Glass and other amorphous materials; (060.2390) Fiber optics, infrared.

References and links

1. P. Kaiser, E. A. J. Marcatili, and S. E. Miller, "A new optical fiber," *Bell Syst. Tech. J.* **52**, 265–269 (1973).
2. P. Kaiser and H. W. Astle, "Low-loss single-material fibers made from pure fused silica," *Bell Syst. Tech. J.* **53**, 1021–1039 (1974).
3. J. C. Knight, T. A. Birks, P. St. J. Russell, and D. M. Atkin, "All-silica single-mode optical fiber with photonic crystal cladding," *Opt. Lett.* **21**(19), 1547–1549 (1996).
4. F. Zolla, G. Renversez, A. Nicolet, B. Kuhlmeiy, S. Guenneau, D. Felbacq, A. Argyros, and S. Leon-Saval, *Foundations of Photonic Crystal Fibres* (Second Edition) (Imperial College, 2012).
5. X. Feng, T. M. Monro, P. Petropoulos, V. Finazzi, and D. Hewak, "Solid microstructured optical fiber," *Opt. Express* **11**(18), 2225–2230 (2003).
6. B. T. Kuhlmeiy, B. J. Eggleton, and D. K. C. Wu, "Fluid-filled solid-core photonic bandgap fibers," *J. Lightwave Technol.* **27**(11), 1617–1630 (2009).
7. A. Argyros, T. A. Birks, S. G. Leon-Saval, C. M. B. Cordeiro, F. Luan, and P. S. J. Russell, "Photonic bandgap with an index step of one percent," *Opt. Express* **13**(1), 309–314 (2005).
8. F. Luan, A. K. George, T. D. Hedley, G. J. Pearce, D. M. Bird, J. C. Knight, and P. S. J. Russell, "All-solid photonic bandgap fiber," *Opt. Lett.* **29**(20), 2369–2371 (2004).
9. J. Troles, Q. Coulombier, G. Canat, M. Duhant, W. Renard, P. Toupin, L. Calvez, G. Renversez, F. Smektala, M. El Amraoui, J. L. Adam, T. Chartier, D. Mechin, and L. Brilland, "Low loss microstructured chalcogenide fibers for large non linear effects at 1995 nm," *Opt. Express* **18**(25), 26647–26654 (2010).
10. M. El-Amraoui, J. Fatome, J. C. Jules, B. Kibler, G. Gadret, C. Fortier, F. Smektala, I. Skripatchev, C. F. Polacchini, Y. Messaddeq, J. Troles, L. Brilland, M. Szpulak, and G. Renversez, "Strong infrared spectral broadening in low-loss As-S chalcogenide suspended core microstructured optical fibers," *Opt. Express* **18**(5), 4547–4556 (2010).
11. J. A. Savage and S. Nielsen, "Chalcogenide glasses transmitting in the infrared between 1 and 20 μm — a state of the art review," *Infrared Phys.* **5**(4), 195–204 (1965).
12. X. H. Zhang, Y. Guimond, and Y. Bellec, "Production of complex chalcogenide glass optics by molding for thermal imaging," *J. Non-Cryst. Solids* **326–327**, 519–523 (2003).
13. G. E. Snopatin, V. S. Shiryaev, V. G. Plotnichenko, E. M. Dianov, and M. F. Churbanov, "High-purity chalcogenide glasses for fiber optics," *Inorg. Mater.* **45**(13), 1439–1460 (2009).
14. L. Calvez, H. L. Ma, J. Lucas, and X. H. Zhang, "Glasses and glass-ceramics based on GeSe₂-Sb₂Se₃ and halides for far infrared transmission," *J. Non-Cryst. Solids* **354**(12-13), 1123–1127 (2008).

15. T. M. Monro, Y. D. West, D. W. Hewak, N. G. R. Broderick, and D. J. Richardson, "Chalcogenide holey fibres," *Electron. Lett.* **36**(24), 1998–2000 (2000).
16. L. Brilland, F. Smektala, G. Renversez, T. Chartier, J. Troles, T. Nguyen, N. Traynor, and A. Monteville, "Fabrication of complex structures of holey fibers in chalcogenide glass," *Opt. Express* **14**(3), 1280–1285 (2006).
17. J. Le Person, F. Smektala, T. Chartier, L. Brilland, T. Jouan, J. Troles, and D. Bosc, "Light guidance in new chalcogenide holey fibres from GeGaSbS glass," *Mater. Res. Bull.* **41**(7), 1303–1309 (2006).
18. J. S. Sanghera, I. D. Aggarwal, L. B. Shaw, C. M. Florea, P. Pureza, V. Q. Nguyen, F. Kung, and I. D. Aggarwal, "Nonlinear properties of chalcogenide glass fibers," *J. Optoelectron. Adv. Mater.* **8**, 2148–2155 (2006).
19. Z. G. Lian, Q. Q. Li, D. Furniss, T. M. Benson, and A. B. Seddon, "Solid microstructured chalcogenide glass optical fibers for the near- and mid-infrared spectral regions," *IEEE Photon. Technol. Lett.* **21**(24), 1804–1806 (2009).
20. M. Liao, C. Chaudhari, G. Qin, X. Yan, C. Kito, T. Suzuki, Y. Ohishi, M. Matsumoto, and T. Misumi, "Fabrication and characterization of a chalcogenide-tellurite composite microstructure fiber with high nonlinearity," *Opt. Express* **17**(24), 21608–21614 (2009).
21. N. Da, L. Wondraczek, M. A. Schmidt, N. Granzow, and P. St. J. Russell, "High index-contrast all-solid photonic crystal fibers by pressure-assisted melt infiltration of silica matrices," *J. Non-Cryst. Solids* **356**(35-36), 1829–1836 (2010).
22. Q. Coulombier, L. Brilland, P. Houizot, T. Chartier, T. N. N'guyen, F. Smektala, G. Renversez, A. Monteville, D. Méchin, T. Pain, H. Orain, J. C. Sangleboeuf, and J. Trolès, "Casting method for producing low-loss chalcogenide microstructured optical fibers," *Opt. Express* **18**(9), 9107–9112 (2010).
23. G. Renversez, F. Bordas, and B. T. Kuhlmeier, "Second mode transition in microstructured optical fibers: determination of the critical geometrical parameter and study of the matrix refractive index and effects of cladding size," *Opt. Lett.* **30**(11), 1264–1266 (2005).
24. L. Brilland, J. Troles, P. Houizot, F. Desevedavy, Q. Coulombier, G. Renversez, T. Chartier, T. N. Nguyen, J.-L. Adam, and N. Traynor, "Interfaces impact on the transmission of chalcogenides photonic crystal fibres," *J. Ceram. Soc. Jpn.* **116**(1358), 1024–1027 (2008).

1. Introduction

The design of silica microstructured optical fibers (MOFs), optical fibers with air holes running along the axial direction, was first demonstrated by Kaiser et al. more than three decades ago [1, 2]. Then, following the successful fabrication of photonic crystal fibers (PCFs) [3], MOFs in which the microstructure is periodic, a wide range of MOFs with different configurations, size and shapes of holes have been elaborated [4]. All-solid MOFs have also been fabricated [5]. This configuration consists in filling the air holes of the microstructure. At least two methods can be considered: incorporating fluids [6] and contrasting refractive index glasses [7, 8]. Band-gap ARROW guiding or more conventional guiding can be obtained in these all-solid MOFs [4].

Non silica based materials such as polymers, lead silicate glasses, tellurite glasses, fluoride glasses, etc have been investigated to design MOFs. Among the soft materials, chalcogenide glasses have been identified as particularly promising candidates for highly non linear applications due to the high non linear index of the materials [9, 10]. Besides, these glasses present a large transparency window. Indeed they can be transparent from the visible region up to the mid infrared depending on the glass composition [11]. They can be shaped as lenses [12], fibers [13], and glass ceramics [14]. The first chalcogenide MOF was proposed by Monro et al. in 2000 [15] and light guidance in chalcogenide glass based MOFs was observed first in 2006 [16–18]. The present paper reports, to the best of our knowledge, the first fabrication of a single mode all-solid chalcogenide glass MOF. Indeed, Lian et al. [19] report a multimode AsSe/GeAsSe fiber and the other reported hybrid fibers are not entirely designed with chalcogenide glasses. As example Liao et al. [20] have realized an As₂S₃/tellurite MOF and Da et al. [21] have elaborated an As₂S₃/silica hybrid MOF. In our study the fiber is based on the As₃₈Se₆₂ glass composition for the matrix and presents three rings of As₂S₃ based inclusions. The refractive indices of the glasses are equal to 2.81 and 2.44 at 1.55 μm for As₃₈Se₆₂ and As₂S₃ respectively. This implies that the guiding type is similar to the one of conventional solid-core MOFs. The guiding properties of the fiber are investigated, and experimental and simulation results are compared.

2. Experimental

2.1. Glass synthesis

The glass rods were fabricated by melting high-purity arsenic and selenium or sulfur together with magnesium metal (Mg) and tellurium tetrachloride (TeCl_4), at 870°C in a vacuum-pumped silica ampoule introduced in a rocking furnace. Magnesium and tellurium tetrachloride act as oxygen and hydrogen getters, respectively. After 10 hours of treatment, the melt was cooled to 700°C and quenched by immersion of the ampoule in water for about 2s. This step is followed by annealing above T_g ($T_g = 165^\circ\text{C}$ and 185°C for $\text{As}_{38}\text{Se}_{62}$ and As_2S_3 respectively).

Then, the prepared glasses were purified by several distillations steps. In the first step, the glasses were distilled under dynamic vacuum. They were heated progressively from 350°C to 450°C to leave behind oxide impurities formed by reaction with magnesium and eliminate gaseous byproducts due to the reaction with TeCl_4 . In the second step, the glasses were distilled under static vacuum in order to eliminate possible remaining oxides. Finally, the distillates were melted again at 870°C for 10 hours, cooled to 650°C , quenched by immersion of the ampoule in water for about 2s and then annealed above T_g .

2.2. As-S/As-Se preform elaboration and microstructured fiber fabrication

The $\text{As}_2\text{S}_3/\text{As}_{38}\text{Se}_{62}$ preform was obtained by a three-step process. First, the As-Se glass rod was molded on a homemade 3 rings of silica capillaries mold as described in [22]. The outer diameter of the resulting preform is 20 mm with holes diameter above $500\ \mu\text{m}$. Secondly, the purified As_2S_3 rod was drawn directly into a $480\ \mu\text{m}$ diameter fiber and the obtained fiber was cut into 6 cm long pieces. Finally, these red As-S sticks have been thread into the holes of the As-Se preform. Pictures of the As-S/As-Se preform obtained are presented in Fig. 1.

The MOF is obtained by drawing the two-glass preform. Spaces between the As-S sticks and the As-Se preform were eliminated upon drawing thanks to a vacuum system.



Fig. 1. $\text{As}_2\text{S}_3/\text{As}_{38}\text{Se}_{62}$ preform: As_2S_3 sticks are thread in the $\text{As}_{38}\text{Se}_{62}$ holey preform.

2.3. Fiber optical characterizations

SEM (Scanning Electron Microscopy) image and EDS (Energy Dispersive Spectroscopy) maps have been achieved on the cross section of the fiber. These sulfur, selenium or arsenic EDS maps allow to visualize the distribution of these chemical elements (Fig. 2).

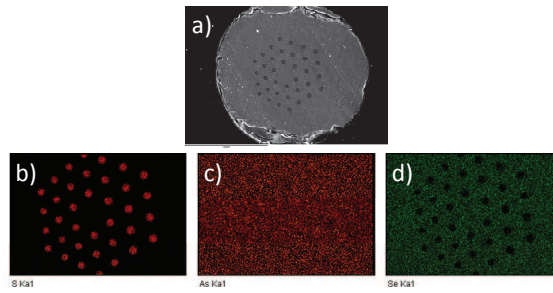


Fig. 2. a) SEM backscattered electrons pictures of the microstructured optical fiber. Picture obtained by b) sulfur c) arsenic and d) selenium detection.

To observe the light guidance a monochromatic light ($\lambda = 1.55 \mu\text{m}$) guided in a single-mode silica fiber was butt-coupled with a 15 cm long chalcogenide MOF. The image of the fiber output was visualized on an IR camera (Fig. 3). In spite of several injection conditions, no modification of the quasi-gaussian mode profile was observed.

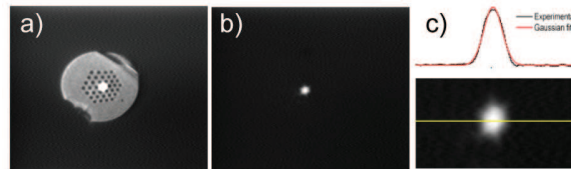


Fig. 3. Near field observation of the 1.55- μm beam at the output of As-S/As-Se MOF a) without and b) with gallium coating and c) Gaussian profile.

In order to evaluate the chemical purity of the glasses, the purified rods were drawn directly as single-index fibers. The optical losses of fibers have been measured on a Bruker Tensor 37 FTIR apparatus with a cooled MCT detector (Fig. 4). The standard cut-back technique was used to determine the attenuation (dB/m). The optical losses of the As-S/As-Se MOF were determined by the same method while a GaSn alloy was applied on the surface of the fiber to inhibit cladding mode guidance (Fig. 4).

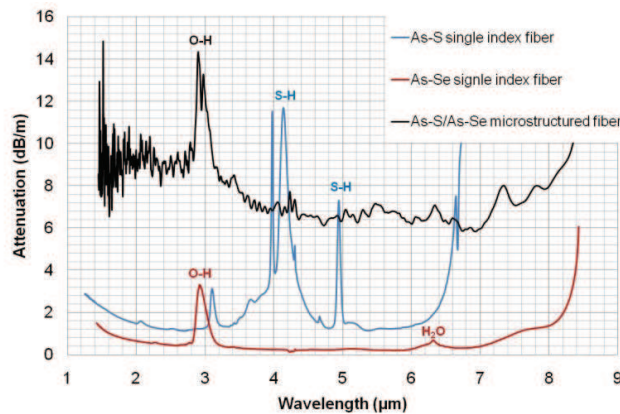


Fig. 4. Optical losses of the As-S single index fiber (blue curve), the As-Se single index fiber (red curve) and the As-S/As-Se microstructured fiber (black curve).

3. All-solid fiber modeling and guiding properties

The theoretical guiding losses and the mode profiles of the elaborated fiber have been investigated using the multipole method [4]. The simulations take into account the fiber parameters and the refractive indices of the two glasses. Using SEM images, the following parameters are found: the averaged high index inclusion diameter d is set to $5.454 \mu\text{m}$, the averaged pitch of the inclusion lattice Λ is set to $14.62 \mu\text{m}$. Consequently the computed d/Λ ratio is equal to 0.373. The MOF is made of $N_r = 3$ rings of inclusions.

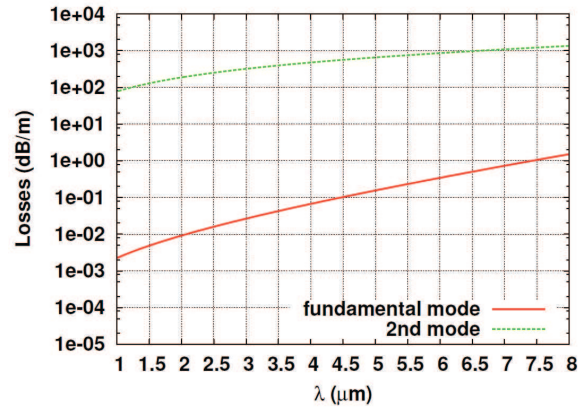


Fig. 5. Theoretical guiding losses (in dB/m with a log scale) versus the wavelength of the all-solid MOF for the fundamental and second modes (fiber parameters are given in the text).

In Fig. 5, both the fundamental mode guiding losses and the second mode ones are given. As it can be seen the fundamental mode losses range from less than 3 dB/km at $1 \mu\text{m}$ to approximately 1.5 dB/m at $8 \mu\text{m}$. In all this wavelength range the fundamental mode is really confined in the fiber core. This result means that in spite of the weak index contrast between the matrix and the inclusions, the operating regime of the fiber corresponds to the low loss “confined fundamental mode” region of this low index inclusion-high index matrix FOM as opposed to the high loss “unconfined fundamental mode” region (see Fig. 8.22 in [4]).

4. Results and discussion

SEM images of the $190 \mu\text{m}$ diameter $\text{As}_2\text{S}_3/\text{As}_{38}\text{Se}_{62}$ MOF obtained are presented in Fig. 2. As expected, As_2S_3 inclusions stand out darker than the $\text{As}_{38}\text{Se}_{62}$ glass on the backscattered electrons picture (Fig. 2(a)). Indeed, sulfur is a lighter chemical element than selenium. By detecting selectively the different chemical elements constituting the fiber we can observe that the arsenic content is almost homogeneous (Fig. 2(c)) in the whole fiber contrary to selenium and sulfur which are precisely localized (Figs. 2(b) and 2(c)).

Near field measurements performed at $1.55 \mu\text{m}$ show a light propagation in the core of the fiber. Figure 3 shows images of the fiber output, without and with gallium layer, as observed on the IR-camera. One can note that the near field measurements indicate a single mode propagation. Figure 5 presents the theoretical losses of the fundamental and the second modes calculated from the geometry of the all-solid fiber. For the second mode the losses range from 100 dB/m at $1 \mu\text{m}$ up to more than 1000 dB/m at $8 \mu\text{m}$. Consequently, from a practical point of view the fabricated fiber can be considered as single mode in the whole wavelength range $1\text{--}8 \mu\text{m}$ because after few centimeters it is not possible to detect a second mode with such high losses. This numerical result is fully coherent with the results on the second mode behavior for low index inclusion-high index matrix MOF [23]. In the present case, due to the low value of N_r , the 2nd mode is not fully delocalized in the microstructure region as it should be with larger N_r value for the obtained $d/\Lambda = 0.373$ which is smaller than the critical d/Λ ratio

estimated to 0.42. We remind that for d/Λ below 0.42 this type of fiber with large Nr is endlessly single mode with a highly lossy and delocalized second mode. One can note that at $1.55\mu\text{m}$ fundamental losses are equal to 5 dB/km while second mode losses reach more than 100 dB/m.

Concerning the chromatic dispersion issue in this MOF, due to the relatively small index contrast between the matrix and the inclusions and to the large core size compared to the studied wavelengths, the chromatic dispersion is fully dominated by the As-Se material chromatic dispersion (simulations not shown). Compared to a MOF with the same geometry and made of an As-Se matrix but with air holes instead of As-S inclusions, the waveguide contribution to the chromatic dispersion of the studied composite MOF is even smaller due to the lower index contrast [4].

It is also worth mentioning that if we have to consider all-solid MOFs with low index inclusions embedded in a high index matrix but with a d/Λ greater than 0.42 then the curve giving the single mode critical wavelength can be estimated quite accurately. One can use the formula (2) of reference [23] without the need for new intensive numerical simulations at least for MOFs with relatively large number of inclusion rings since this formula depends explicitly on the inclusion and matrix refractive indices.

Optical losses of the As-S/As-Se microstructured fiber are shown in Fig. 4, together with the optical attenuation of As-S and As-Se bulk glasses, for comparison. Before the elaboration of the all-solid MOF, optical losses are around 0.5 dB/m and 1.2 dB/m at $2.5\mu\text{m}$ for the AsSe and the AsS glass respectively. It is observed that optical losses increase by more than 6-7 dB/m in the range 1-8 μm , for the microstructured fiber as compared to the As-Se bulk glass. As shown in Fig. 5 the theoretical losses of the fundamental mode of the MOF are much lower than the experimental losses. For instance, at $2\mu\text{m}$ theoretical losses are as low as 0.01dB/m while the measured global fiber losses are about 9 dB/m. Optical losses of the fiber are higher than the sum of material and theoretical losses. These high losses of the fabricated fiber are consequently due to the casting process which leads to defects at the glass interface regions. Indeed, an optical microscope observation (not shown) reveals air bubbles at the interfaces between the two materials. Brilland et al. [24] have already demonstrated that defects at the glass interface regions generate excess of losses. Besides, the O-H absorption band at 2.9 μm is more intense for the microstructured fiber than for the As-Se single index fiber. This increase can be due to water pollution during the molding process. However, the results show that the chemical purity of the glass inclusions does not impact on the optical losses of the all-solid MOF. Indeed, the hydrogen impurities, leading to S-H absorption bands, present in the As_2S_3 bulk glass are not visible on the attenuation curve of the microstructured fiber core. This absence of the S-H absorption band shows a good light confinement in the AsSe fiber core.

5. Conclusion

This study reports the first realization of a single mode all-solid chalcogenide microstructured optical fiber. The glass matrix of the fiber is based on the $\text{As}_{38}\text{Se}_{62}$ composition and the As_2S_3 glass has been used as low index inclusions. The fiber presents 3 rings of inclusions. The diameter of the As_2S_3 inclusions is approximately 5.4 μm and the fiber core diameter is around 24 μm . The performed fiber shows a single mode light propagation which can be explained by the strong losses of the second mode. Optical transmission measurement of both the microstructured fiber and single index fiber reveal an excess of losses as high as 6-7 dB/m. This excess of optical losses is not due to the guide geometry but it is explained by the presence of defects in the glass interface regions.

Acknowledgments

The authors acknowledge the French Délégation Générale pour l'Armement for its financial support.